

Leibniz-Institut für Astrophysik Potsdam	OH-SUPER Final Report	Friedrich-Schiller-Universität Jena
---	--------------------------	--

FINAL REPORT

1 General Information

Project number:	455425131
Project title:	Next Generation OH Suppression Fiber Bragg Gratings: towards Operation on Sky
Principle Investigator:	Prof. Dr. Martin M. Roth (2021-2022) Dr. Aashia Rahman (2022-2025) Leibniz-Institut für Astrophysik Potsdam (AIP) Potsdam
Principle Investigator:	Prof. Dr. Stefan Nolte Friedrich-Schiller-Universität Jena (Uni Jena) Institut für Angewandte Physik Jena
Reporting period:	01.01.2021 - 31.05.2025

2 Summary

English Version

Near-infra red (NIR) ground based astronomical observations suffer from the existence of bright and dense hydroxyl (OH) emission lines [Meinel, ApJ 112 (1950)] originating in the earth's atmosphere. Suppression of OH lines will be a crucial aspect in the upcoming generation of extremely large telescopes operating at the NIR, e.g., Extremely Large Telescope (ELT). GNOSIS and PRAXIS instruments successfully demonstrated [Trinh et al., The Astron. J. 145 (2013), Ellis et al., MNRAS 492 (2020)] the capability of fiber Bragg grating (FBG) filter technologies to suppress the OH lines by factors of 8 to 9.

In the OH-SUPER project, Leibniz Institute for Astrophysics Potsdam (AIP) and the Friedrich-Schiller-University Jena (Uni Jena) collaborated to investigate and develop new inscription techniques and design approaches for manufacturing these filters. Using ultraviolet (UV) laser, AIP established a running light interferometry system, to inscribe up to 15 cm long, multi-notch filters, for a maximum 22 nm bandwidth. This setup is promising and lays the groundwork for future efforts to inscribe repeatable multi-notch filters. AIP also explored novel phase mask designs for inscription of 5 filter lines using UV laser and investigated improving the precision of the target wavelengths. Uni Jena explored scaling aperiodic FBGs up to 20 notches based on the line-by-line method using femtosecond infrared laser (fs-IR). Furthermore, Uni Jena conceptualised and developed a novel "shape aperture" method for inscription of repeatable, spectrally tailored filters using a phase mask method. Evaluation of throughput showed phase mask fs-IR FBG in SMF-28 fiber outperforming UV-inscription into photosensitive fibers. As a result, 7 sets of identical 20-notch filters were realized by the fs-IR phase mask technique at Uni Jena with an excellent interline throughput of at least 93%. AIP developed an athermal

Leibniz-Institut für Astrophysik Potsdam	OH-SUPER Final Report	Friedrich-Schiller-Universität Jena
---	--------------------------	--

packaging solution, stabilizing the filter lines against temperature variations, achieving a maximum wavelength deviation of 12 pm over a temperature range from -17°C to 15°C. Finally, laboratory based short-term stability of the filters was investigated and a trial run with the astrophotonic spectrograph at AIP based on arrayed waveguide grating (the Potsdam arrayed waveguide Spectrograph, PAWS) was performed, jointly by AIP and Uni Jena.

This research project has significantly advanced the capability of low-loss OH line filter realization, laying the foundation for efficiently scaling the OH-line suppression capacity. Furthermore, advances in packaging and instrumentation allows for the development of an efficient prototype all-astrophotonic instrument, to advance the field of astrophotonics for future ground-based telescopes benefiting the astronomical community.

German Version

Astronomische Beobachtungen von der Erde aus im nahen infraroten Wellenlängenbereich (NIR) werden durch helle und dichte Hydroxyl (OH)-Emissionslinien beeinträchtigt, die aus der Erdatmosphäre stammen (Meinel, ApJ 112 (1950)). Die Unterdrückung der OH-Linien wird ein entscheidender Aspekt bei Teleskopen der kommenden Generation sein, die im NIR arbeiten, wie z.B. beim Extremely Large Telescope (ELT). Die Instrumente GNOSIS (Trinh et al., The Astron. J. 145 (2023)) und PRAXIS (Ellis et al., MNRAS 492 (2020)) haben bereits gezeigt, dass Filtertechnologien basierend auf Faser-Bragg-Gittern (FBG) in der Lage sind, OH-Linien um den Faktor 8 bis 9 zu unterdrücken.

Im Rahmen des OH-SUPER-Projekts haben das Leibniz-Institut für Astrophysik Potsdam (AIP) und die Friedrich-Schiller-Universität Jena (Uni Jena) gemeinsam neue Techniken und Designs für die Realisierung dieser Filter untersucht und entwickelt. Dabei wurde unter Verwendung eines ultravioletten (UV-) Lasers am AIP "running light" Interferometrie etabliert, um bis zu 15 cm lange Mehrfach-Notch-FBG über eine Bandbreite bis zu 22 nm zu erzeugen. Die Entwicklungen legen den Grundstein für das reproduzierbare Einschreiben von Mehrfach-Notch-Filtern. Am AIP wurden weiterhin neuartige komplexe Phasenmaskendesigns für die Erzeugung von 5-Notch-Filtern mittels UV-Laser entwickelt und Methoden zur Genauigkeit der Zielwellenlänge untersucht. Die Uni Jena erforschte die Skalierung aperiodischer FBG auf bis zu 20 Notches auf Basis der Line-by-Line-Methode unter Verwendung eines Femtosekunden-Infrarotlasers (fs-IR). Außerdem entwickelte die Uni Jena die neuartige "shaping aperture"-Methode, mit der mittels Phasenmaskentechnik spektral angepasste Filter reproduzierbar hergestellt werden können. Die Evaluierung der Filterverluste zeigte, dass die Phasenmasken-fs-IR-FBG die Performance der UV-eingeschriebenen FBG deutlich übertrifft. Demzufolge wurden 7 Sätze identischer 20-Notch-Filter mit einer Effizienz von mindestens 93% mittels der fs-IR Phasenmaskentechnik an der Uni Jena realisiert. Das AIP entwickelte

Leibniz-Institut für Astrophysik Potsdam	OH-SUPER Final Report	Friedrich-Schiller-Universität Jena
---	--------------------------	--

ein athermisches Gehäuse, das die Filter gegen Temperaturschwankungen stabilisiert und eine maximale Wellenlängenabweichung von 12 pm über einen Temperaturbereich von -17°C bis 15°C erreicht. Schließlich wurde die Kurzzeitstabilität der Filtersätze im Labor gemeinsam vom AIP und der Uni Jena untersucht, und ein Testlauf mit dem hauseigenen (AIP) astrophotonischen Spektrograf auf Basis eines "Arrayed Waveguide Grating" (PAWS) durchgeführt.

Dieses Forschungsprojekt hat die Techniken zur Realisierung verlustarmer OH-Linienfilter erheblich weiterentwickelt und damit die Grundlage für eine effiziente Skalierung der OH-Linienunterdrückungskapazität geschaffen. Darüber hinaus ermöglichen Fortschritte in Stabilisierung und Instrumentierung die Entwicklung eines effizienten astrophotonischen Prototyps, um das Gebiet der Astrophotonik für zukünftige bodengestützte Teleskope voranzubringen.

3 Detailed Description

In next-generation extremely large telescopes (e.g., the ELT), NIR astronomy will drive major advances for science cases, such as, e.g., exoplanets, dark matter, dark energy, black holes, formation and evolution of galaxies, and a view into the earliest ages of the Universe, the Epoch of Reionisation. Ground-based NIR observation is challenged due to the existence of dense and bright hydroxyl (OH) emission lines in the Earth's atmosphere. These lines, beginning near 610 nm and extending to 2.62 μm with peak intensity around 1500 nm, are several orders of magnitude stronger [Rou00] than faint astronomical signals. They generate substantial stray light within spectrographs and fluctuate rapidly in intensity, making subtraction methods unreliable. Since OH lines are narrow (tens of pm) and fixed in wavelength, pre-spectrograph filtering is highly effective. Fiber Bragg gratings (FBGs), which act as narrowband reflectors through periodic refractive index modulation, are ideal for this purpose and have been demonstrated successfully [Eil2020]. To advance and further establish the technology for low-loss and efficient OH-line suppression instrumentation, AIP and Uni Jena collaborated in this project with an objective to develop and investigate two complementary FBG fabrication approaches: ultraviolet (UV) inscription using phase mask and interferometric techniques at AIP, and femtosecond-infrared (fs-IR) direct writing as well as using phase mask techniques at Uni Jena. Alongside filter development, both partners worked on novel phase mask development, photonic lanterns, and temperature-compensating packaging solutions. Finally, for performance study of the filters, an on-sky demonstrator that includes the filters was to be developed and integrated.

UV Running light interferometry

AIP established a UV-running light interferometry system equipped with electro-optic phase modulators (EOMs) for inscribing long (10 cm to 15 cm), aperiodic FBG (aFBG) filters with bandwidths up to 22 nm. In this setup, we investigated several aspects, e.g., (a) stability, (b) fiber core tracking and correcting setup (FTCS) [Gün2023], (c) alignment and characterisation of EOMs, (d) minimising unwanted residual amplitude modulation to establish such an advanced FBG inscription facility. With successful alignment and mitigation of several experimental challenges, 10 -15 cm FBG filters were inscribed. For example, Fig. 1 shows the reflection spectrum obtained from an aperiodic three notch FBGs inscribed using this setup.

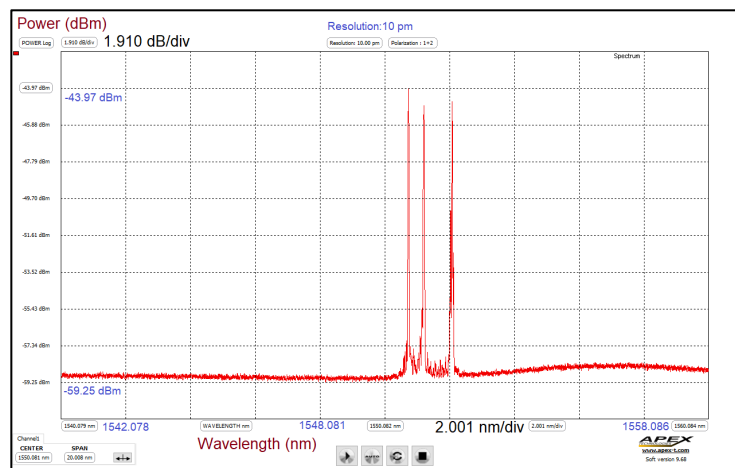


Figure 1. Reflection spectrum of a 3-notch aFBG filter fabricated by tuning the EOM input parameters @AIP, the wavelengths of the three notches are 1552.13 nm, 1551.25 nm, 1550.78 nm.

Furthermore, multi-notch filters with up to 11 notches could be fabricated by varying the input frequency (f_{EOM}) while translating the fiber at constant speed. More complex filters can be fabricated using a pre-programmed varying f_{EOM} for a given spot size and fiber speed. However, reducing the spot size to extend the bandwidth requires a two-plane fiber position monitoring system to ensure repeatability. The procurement of such a system was out of the scope in this project. Consequently, full mitigation of repeatability challenges was not achieved within the current timeframe, and the full potential of this technique for OH line filters remains unexplored. Nonetheless, the demonstrated capability establishes a foundation for future efforts toward fabricating repeatable multi-notch aFBGs and ultimately determining the interline throughput.

UV phase mask

At AIP, we explored complex phase mask (CPM) to inscribe the complex OH filters. The first

generation CPM [Rah2020] was based on phase sampling. It was experimentally observed that the first-generation CPM produced noisy reflection spectra. This was due to two reasons – a) no amplitude modulation was possible, b) phase sampling period of 10 mm requires strict fiber positioning with respect to the CPM. Therefore, a new concept was developed. As proof-of-concept, two phase masks were designed at AIP and fabricated by Uni Jena [Rah2023, Luo2024] for notch #3 to #7 [Appendix A], first one with individual gratings shifted laterally with group delays (PM1 in Fig. 2a) [Ska2003, Bur2003]; and the second one where all the shifted gratings were overlapped into a single continuous mask, with logical OR and XOR operation (PM2 in Fig. 2a) in the overlap locations. OR logical operation showed promising results, although more investigation is warranted. Figure 2b shows the transmission spectra of the 5 notches inscribed with PM1, a high precision to target wavelengths were achieved.

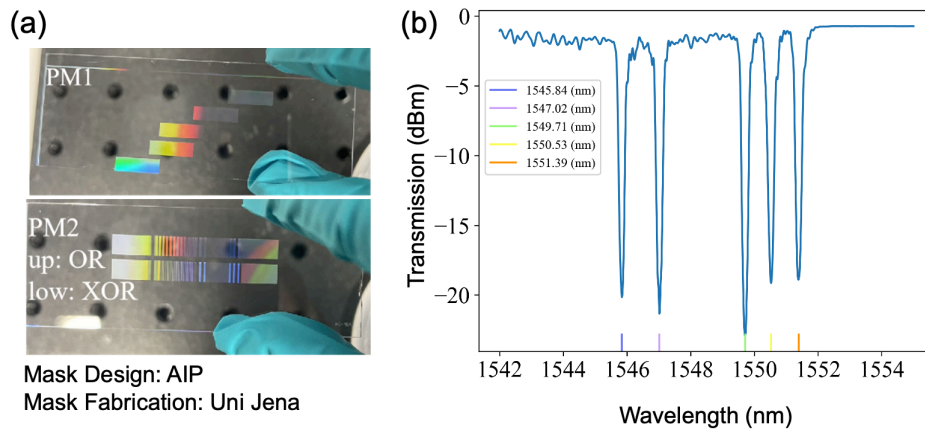


Figure 2. (a) PM1: individual gratings with group delays. PM2: overlap of the individual gratings using OR and XOR logical operations. (b) Transmission spectra of the 5-notch FBG filters.

fs-IR written multi-notch aperiodic fiber Bragg gratings

Uni Jena continued their work on the fs-IR-laser inscription of aperiodic fiber Bragg gratings (aFBG), providing a multi-notch filter, based on the line-by-line technique [Goe2018]. The aim was to increase the previously demonstrated number of notches from 10 to 20 (see Fig. 3a). Even though all spectral resonances were close to their target, the transmission spectrum showed still significant broadband losses up to -3 dB (50%) due to scattering and absorption, cladding mode coupling as well as intermediate peaks caused by the initial design. To provide a more stable, low-loss and faster inscription of aFBG, the implementation of aperiodic phase masks was investigated. This would offer the utilization of the phase mask scanning technique, where the phase mask (diffraction grating) generates a two-beam interference pattern, which is imprinted into the fiber core using a cylindrical lens [Tho2012]. Since an aFBG requires a complex period distribution, the challenge is designing phase mask sections, ensuring the overlap of their diffracted beams generates the desired interference pattern. A basis for this work has been presented in [Goe2020], where consecutively FBGs of few mm length were

realized. An aFBG requires a minimalization of the individual grating sections into the range of a few micrometers (see Fig. 3b). The phase mask was realized and probed for FBG inscription. However, the margin for error in fiber positioning and alignment proved too critical and no formation of resonances was observed, which requires further investigations.

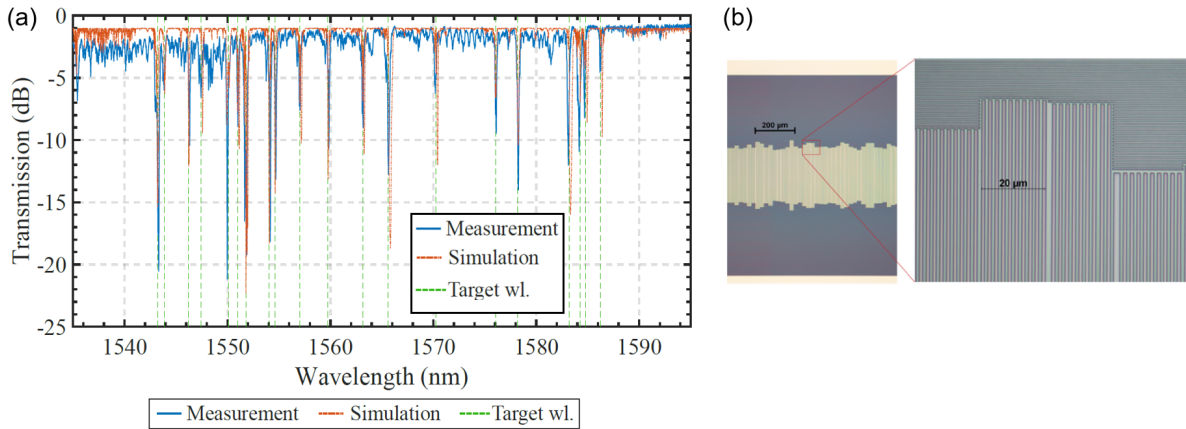


Figure 3. (a) Simulated (red) and measured (blue) transmission spectrum of a fs-IR-inscribed aFBG providing 20 notches. (b) Microscope images of aperiodic phase mask.

fs-IR-written single notch FBG based on phase mask aperture shaping

In another approach, Uni Jena developed a tool for flexible shaping the spectral response using the standard fs-IR phase mask inscription technique for single notch FBG, based on shaping apertures, which is presented in [Krä2022, Krä2023, Krä2025a]. For a more reliable and repeatable inscription, this shaping aperture was directly implemented into the phase mask (see Fig. 4a) [Krä2025b]. A mask providing the inscription of 20 notches with individual designs matched to selected OH-emission lines, was realized. During inscription, the FBG were grouped into 5 sets of each 4 consecutive FBG within a 50 mm inscription window, overall reproduced into 7 fibers (SMF-28). To ensure repeatability, image recognition-based alignment options and fiber strain control have been implemented into the inscription setup. Fig. 4b demonstrates good matching of the targeted spectral shape concerning bandwidth and strength, as well as the repeatability of the inscription process with average deviations below 60 pm and 7% for resonance wavelength and bandwidth, respectively (see Appendix A for details). To provide long term stability and mitigate degradation effects of the refractive index modification, all FBG sets were annealed at 300°C for 10 min. This led as well to a reduction of broadband losses caused by absorption or scattering.

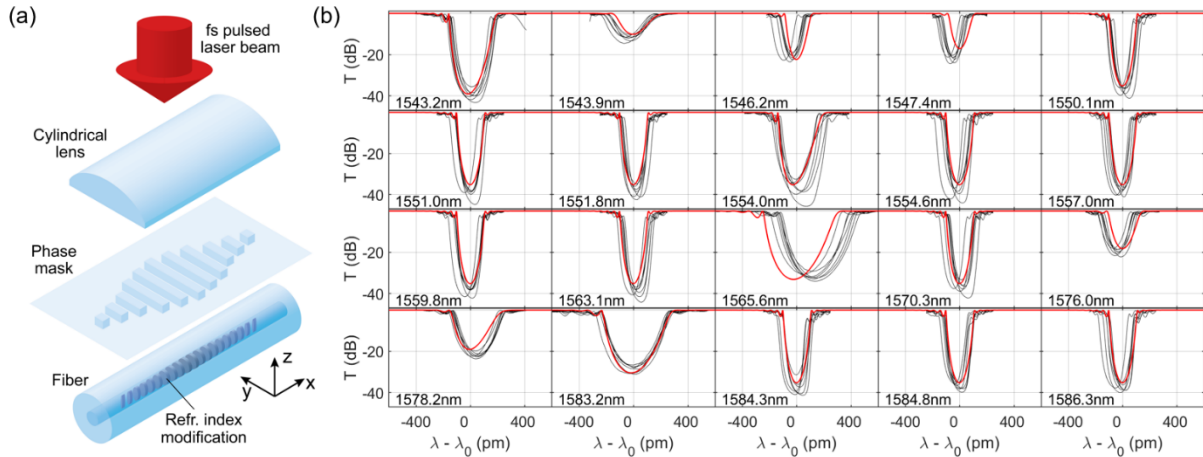


Figure 4. (a) Sketch of phase mask inscription with integrated shaping aperture. (b) Measured (black) and simulated (red) transmission spectra of the 20 notches each inscribed into 7 different fibers [Krä2025b].

Phase mask development and accuracy of resonance wavelength

The phase masks for UV and femtosecond-laser inscription were fabricated at Uni Jena using variable-shape electron-beam lithography (Vistec SB350OS) followed by ICP etching of fused silica. A fundamental limitation of serial e-beam patterning is the discrete address grid, eventually constraining the spectral resolution. Within this project, we refined a super-sampling method [Heu2025], achieving an effective 0.1 nm resolution. Thereby, enabling phase-mask technology for OH-emission line filtering.

Phase mask periods are determined under consideration of the effective refractive index of the optical fiber for inscription for a given set of inscription parameters. It must be considered that various types of fibers, such as different photosensitive fibers evaluated for inscription at AIP, show different refractive indices of the core. Also, different batches of similar fiber, or different inscription parameters (e.g. long and weak vs. strong and short FBG), cause a deviation of the effective refractive index of the fiber core mode. To correct for the desired resonance wavelength, there are two approaches: during the inscription process, the fiber is pre-strained specifically based on its stress-optic coefficient, providing a targeted resonance wavelength shift to lower wavelengths upon releasing the fiber afterwards [Luo2025a]. Alternatively, Uni Jena investigated post-processing, increasing the refractive index within the fiber core in the grating area, thereby increasing the resulting resonance wavelength [Imo2021, Goe2021]. Both techniques are applicable for single FBG within larger arrays.

Loss evaluation of UV- and fs-IR based inscription

There are mainly three sources of loss: broadband losses due to absorption or scattering at the refractive index modification, coupling loss to SMF-28-based surrounding instrumentation, as well as interline loss due to coupling to cladding modes (CM). For reduction of CM losses, AIP examined three fibers: a low numerical aperture photosensitive fiber (PS1250:Fibercore),

a highly photosensitive fiber (SM1500:Fibercore) and a cladding mode suppressed fiber (GF4A:Thorlabs). UV inscription employed the above-mentioned complex phase mask [Luo2024]. To complete the comparison, Uni Jena provided fs-IR aperture phase mask inscribed FBG in SMF-28 fiber. Fig. 5 shows transmission spectra of 5-notch FBG arrays in all 4 different fiber types. Whereas CM loss could be strongly reduced in SM1550 and GF4A, UV-inscribed photosensitive filter fibers show much higher broadband losses caused by absorption and especially coupling losses due to mode field mismatch to SMF-28 (see full table in Appendix B). Since fs-IR phase mask FBG showed higher potential for low-loss filters, this technique was further pursued for realization of the final filter elements.

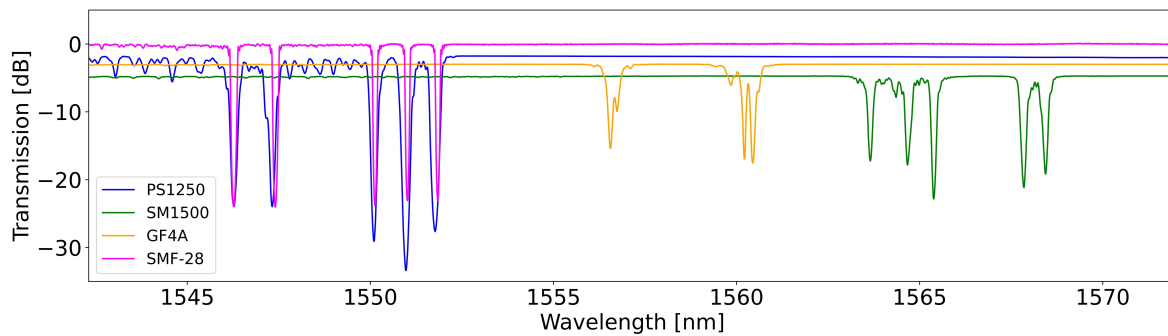


Figure 5. Comparison of transmission loss for UV- and fs-IR inscription (SMF-28) for different fiber types.

Athermal package development & characterisation



Figure 6. Athermal package.

Beyond the results of fabrication methods and their accuracies described above, post-fabrication packaging to stabilize the filters during operation is critical. At AIP we designed [Alv2024a, Alv2024b], manufactured, and characterized [Luo2025b] an athermal package (Fig. 6) to accommodate 11 cm of optical fiber consisting of FBG filters. The athermal package demonstrated

a maximum wavelength deviation of 12 pm, over the temperature range from -17°C to 15°C . A critical design step was determining the strain and temperature sensitivities of the fibers used at AIP and Uni Jena. These parameters were used in designing the package, resulting in two units—one for AIP filters and one for Uni Jena filters. Each package accommodated 5-notch FBG arrays. The design remains flexible and can be readily scaled to longer fiber lengths or to integrate multiple fiber loops.

Photonic lantern

AIP houses a photonic lantern fabrication facility that has produced one multimode fiber (MMF)-to-seven single mode fiber (SMF) photonic lanterns for several projects, including OH-SUPER. Rypalla et al. [Ryp2024] demonstrated repeatability of the process through mass

production and characterization achieving throughput exceeding 30% for MMF-7xSMF-MMF lantern device. Given the consistent production capability at AIP, multiple lanterns with repeatable throughput can be employed, scaling to 1 to 19 or higher PL devices, in future for a complete OH line FBG filter demonstrator.

Integration with PAWS spectrograph

As part of the instrumentation, we finally integrated the filters and photonic lanterns with an in-house (@ AIP) developed astrophotonic spectrograph, Potsdam Arrayed Waveguide Spectrograph (PAWS) [Her2022]. The resolving power ($\Delta\lambda/\lambda$) of PAWS is approx.10,000. In this project, we re-calibrated PAWS in May 2025 using a tuneable laser source, confirming that it has maintained stable spectral performance with no variation over 2+ years of operation since its commissioning in 2023. In Fig. 7, we present the filters (AIP and Uni Jena filters) as observed using the PAWS spectrograph.

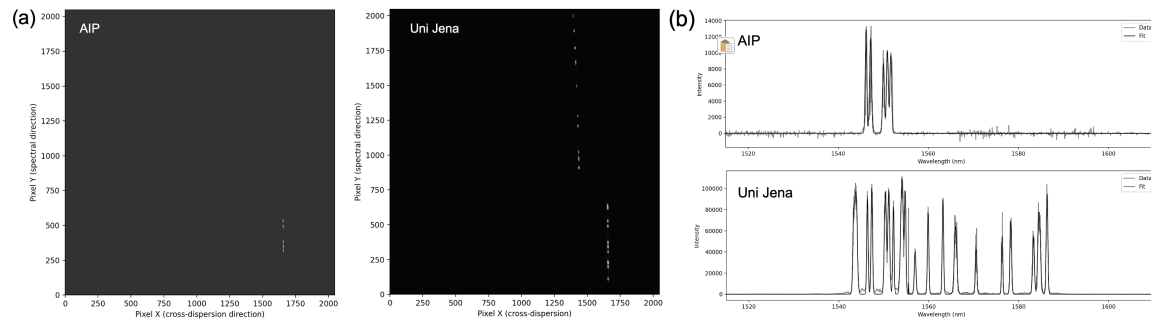


Figure 7. (a) The PAWS spectrograph frames and (b) the corresponding FBG filter spectra.

Assembly of notch filters with athermal package

Eventually, the final filter device consisting of the fs-IR phase mask written FBG was to be assembled and tested in a joint short term stability measurement by AIP and Uni Jena. A 4-FBG array of one 20-FBG set was placed and glued into the athermal package. The other arrays were glued onto a test stage with optional application of strain for resonance wavelength correction. All were fixed to an optical table and the transmission spectra were recorded overnight (see Fig. 8). As expected, the resonance wavelength of the test stage FBGs drifted with the temperature. However, much stronger (50 K/pm instead of 11 K/pm), possibly due to additional mechanical stress of the test stage. The resonance of the athermal package FBGs behaved in an opposite way, where the athermal package was overcompensating the temperature drift, showing as well large wavelength shifts (-30 pm/K). This behavior is most likely due to the issues discussed in [Luo2025b], where temperatures above the dew point, which was $<17^{\circ}\text{C}$ in this measurement, compromised the performance of the adhesive fixing the fiber in the package, which requires further investigations. However, the bandwidth and transmission loss showed only negligible deviations.

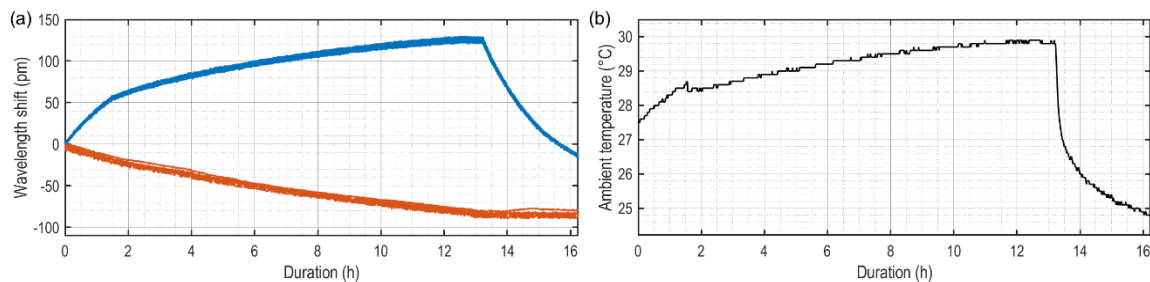


Figure 8: (a) Shift of center resonance wavelength of 20-FBG array placed in athermal package (red) and test stage (blue). (b) ambient temperature over 16 hours.

Throughput performance of 20-notch filter sets

Exemplary, Fig. 9 shows the full transmission spectrum of Set #2. A detailed chart of targeted values and measured results for all sets is given in Appendix A. Broadband losses caused by absorption or scattering (measured at the long wavelength side) are estimated to less or equal to approx. 3%. The overall throughput, additionally affected by cladding mode losses, is at least 93%. In comparison, [EII2020] has stated for the FBG unit of PRAXIS consisting of 103 notches a relative throughput of 39%. The expected throughput for a factor 5 more notches/FBG with the fs-IR phase mask inscription would be estimated to 65% with the current results. This would suggest a significant improvement to the published work.

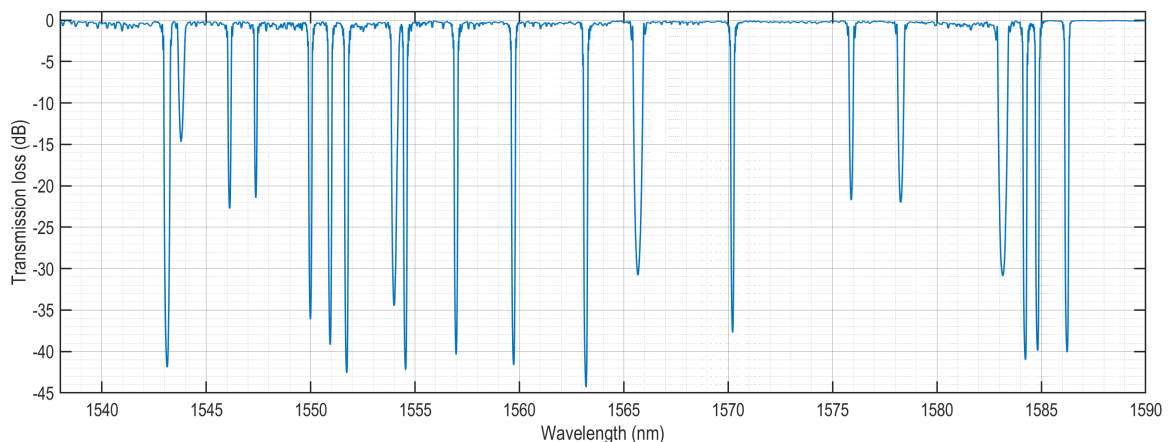


Figure 9. Full transmission spectrum of one final fs-IR-written 20-FBG array.

Conclusions

In this work, multiple approaches for fabricating and implementing FBG-based filters were explored. At AIP, UV running-light interferometry was established for inscribing aperiodic complex filters, with repeatability challenges identified for future improvement. Novel UV complex phase mask concepts enabled repeatable five-notch arrays with controlled group delays. At Uni Jena, line-by-line inscription of aperiodic FBG was scaled up to 20 notches, though with significant interline losses. A phase mask method with aperture shaping was subsequently developed, providing low-loss, repeatable notches with tailored spectra. Fiber

Leibniz-Institut für Astrophysik Potsdam	OH-SUPER Final Report	Friedrich-Schiller-Universität Jena
---	--------------------------	--

loss characterization showed fs-IR inscription outperforming UV, and post-processing annealing enhanced performance. Finally, seven 20-notch filter sets with excellent interline throughput of 93% were realized. On the instrumentation side, AIP fabricated repeatable photonic lanterns and developed an athermal packaging solution to ensure long-term stability. Short-term stability tests were conducted, and packaged filters have now been integrated with an astrophotonic spectrograph via photonic lanterns to enable future long-term studies. Collectively, advances in filter fabrication, packaging, and system integration establish a strong foundation for stable, scalable, and efficient astrophotonic instrumentation for ground-based telescopes.

4 Published Project Results

4.1 Category A

Publications in scientific peer-reviewed journals:

- [Goe2021] T. A. Goebel, J. Nold, C. Hupel, S. Kuhn, N. Haarlammert, T. Schreiber, C. Matzdorf, T. O. Imogore, R. G. Krämer, D. Richter, A. Tünnermann, and S. Nolte, "Ultrashort pulse written fiber Bragg gratings as narrowband filters in multicore fibers," *Applied Optics* 60, D43 (2021). doi.org/10.1364/AO.421089 (open access)
- [Krä2025a] R. G. Krämer, C. Schmittner, T. Ullsperger, M. P. Siems, S. L. Döpfner, G. R. Schwartz, D. Richter, and S. Nolte, "Shaping the spectral response of ultrashort pulse phase mask written fiber Bragg gratings," *Opt. Express* 33, 28152 (2025). doi.org/10.1364/OE.558398 (open access)
- [Luo2025b] X. Luo, C. E. R. Alvarez, A. Rahman, A. A. Soemitro, H. Önel, J. Paschke, S-M. Bauer, K. Madhav, W. Bittner, and M. M. Roth, "Temperature-compensating package for OH line filters for astronomy: II. manufacture, assembly, and performance study," *Opt. Express* 33, 34008-34029 (2025). doi.org/10.1364/OE.560633 (open access)

Contributions to peer-reviewed conferences:

- [Imo2021] T. O. Imogore, T. A. Goebel, R. G. Krämer, C. Matzdorf, D. Richter, and S. Nolte, "Femtosecond laser post-processing mechanisms for refractive index tuning of fiber Bragg gratings," in *Frontiers in Optics + Laser Science 2021*, p. JW7A.98 (2021). doi.org/10.1364/FIO.2021.JW7A.98
- [Krä2022] R. G. Krämer, C. P. Schmittner, T. A. Goebel, M. P. Siems, T. Ullsperger, T. O. Imogore, D. Richter, and S. Nolte, "Tailored Apodization of Femtosecond Written Fiber Bragg Gratings by Aperture Shaping," in *Optica Advanced Photonics Congress 2022*, p. BTu1A.5 (2022). doi.org/10.1364/BGPPM.2022.BTu1A.5
- [Krä2023] R. G. Krämer, C. P. Schmittner, M. P. Siems, T. Ullsperger, T. A. Goebel, D. Richter, and S. Nolte, "Ultrashort pulse inscribed fiber Bragg gratings with controlled apodisation profiles," in *Components and Packaging for Laser Systems IX*, (SPIE, 2023), p. 5. doi.org/10.1117/12.2649952
- [Rah2023] A. Rahman, T. Siefke, K. Madhav, T. A. Goebel, A. Ghazagh, U. D. Zeitner, X. Luo, D. Richter, S. Nolte, and M. M. Roth, "Design and fabrication of a novel phase mask to inscribe fiber Bragg gratings for astronomical applications," in *CLEO 2023, Technical Digest Series* (Optica Publishing Group, 2023), paper SF1H.3. doi.org/10.1364/CLEO_SI.2023.SF1H.3
- [Luo2024] X. Luo, A. Rahman, K. V. Madhav, T. Siefke, R. G. Krämer, D. Richter, U. D. Zeitner, S. Nolte, and Martin M. Roth, "Novel phase masks with overlapping regions to fabricate fiber Bragg gratings for filtering sky emission lines," *Proc. SPIE 13100, Advances in Optical and*

Leibniz-Institut für Astrophysik Potsdam	OH-SUPER Final Report	Friedrich-Schiller-Universität Jena
---	--------------------------	--

Mechanical Technologies for Telescopes and Instrumentation VI, 1310068 (2024).

doi.org/10.1117/12.3018363

[Alv2024a] C. E. R. Alvarez, A. Rahman, H. Önel, F. Dionies, J. Paschke, and S-M. Bauer, "Athermal package for OH suppression filters in astronomy - part1: design," Proc. SPIE 13100, Advances in Optical and Mechanical Technologies for Telescopes and Instrumentation VI, 131002H (2024). doi.org/10.1117/12.3017699

[Krä2025b] R. G. Krämer, S. L. Döpfner, M. P. Siems, G. R. Schwartz, D. Richter, and S. Nolte, "Phase Mask Integrated Aperture Shaping for Efficient Writing of Multiple Notch Filters in the Form of Fiber Bragg Gratings," 2025 CLEO/Europe-EQEC, Munich, CM-P.8, Germany (2025) doi.org/10.1109/CLEO/Europe-EQEC65582.2025.11110367

[Luo2025a] X. Luo, A. Rahman, A. M. Weiß, K. Madhav, and M. M. Roth, "Fabrication of Precise Fiber Bragg Grating Filters for Astronomy," 2025 CLEO/Europe-EQEC, Munich, CE-1.5, Germany (2025) doi.org/10.1109/CLEO/Europe-EQEC65582.2025.11111190

Publications accepted or in preparation:

[Heu2025] M. Heusinger, T. A. Goebel, M. Banasch, D. Richter, R. G. Krämer, C. Voigtländer, E. Linn, T. Siefke, A. Tünnermann, E.-B. Kley, S. Nolte, U. D. Zeitner, "Sub-nanometer address grid in variable shaped e-beam lithography for efficient inscription of high-precision large-area optical gratings", submitted to Photonics Research, accepted, Manuscript ID 541297.

4.2 Category B

Graduation thesis:

Z. Lin, "Phase-Shifted Fiber Bragg Gratings via Localized Femtosecond Photo-Treatment", Master's Thesis, Friedrich-Schiller-Universität Jena, 2022

S. L. Döpfner, "Lifetime Characterization of Ultrashort Laser Pulse Written Fiber Bragg Gratings," Bachelor's Thesis, Friedrich-Schiller-Universität Jena, 2023

C. E. R. Alvarez, "Entwicklung und Untersuchung eines Temperaturkompensators für Faser Bragg-Gitter zur Anwendung in der Astronomie," Master's Thesis, Technische Universität Berlin, 2024

Dissertation:

T. A. Goebel, "Multi-Channel spectral filtering by femtosecond written fiber Bragg gratings," Dissertation, Friedrich-Schiller-Universität, 2022

T. O. Imogore, "Spectral and dispersion tuning of fiber Bragg gratings by tailored femtosecond laser refractive index modification," Dissertation, Friedrich-Schiller-Universität Jena, 2025

4.4 Patents (applied for and granted)

[Gün2023] A. Günther, "Method and control system for controlling a process for writing gratings into an optical fiber," EP3988973B1, Granted on 11.10.2023.

[Alv2024b] C. E. R. Alvarez, A. Rahman, H. Önel, F. Dionies, J. Paschke, "Optisches Filtersystem zur Wellenlängenfilterung," Filed on June 20, 2024.

Appendix A – Chart list of filter parameters

Table 1. Targeted wavelength, transmission loss (T) and bandwidth (full width at half maximum) for 20 selected OH-lines (selected from [Rou2000]), as well as measured values of all 7 filter sets.

Resonance #	Unit	1	2	3	4	5	6	7	8	9	10	11	12	13	14	15	16	17	18	19	20
Target																					
Wavelength	nm	1543.203	1543.861	1546.214	1547.423	1550.088	1550.979	1551.788	1554.035	1554.615	1557.018	1559.764	1563.134	1566.625	1570.254	1576.03	1578.21	1583.179	1584.252	1584.807	1586.253
Transmission	dB	-39	-9	-22	-17	-35	-35	-35	-35	-35	-35	-35	-35	-33	-35	-16	-19	-30	-35	-35	-35
Bandwidth	pm	330	260	180	165	200	200	200	310	200	200	200	200	520	200	220	330	480	200	200	200
Filter set #1																					
Performance			Broadband loss	2.9%		Interline Throughput		93%		Avg. absolute wavelength dev.			32 pm		Avg. relative bandwidth dev.			5%			
Wavelength	nm	1543.235	1543.840	1546.185	1547.353	1550.125	1550.990	1551.830	1554.083	1554.615	1557.018	1559.780	1563.170	1566.783	1570.293	1576.018	1578.253	1583.190	1584.258	1584.778	1586.258
Transmission	dB	-40.3	-14.0	-21.0	-24.8	-41.9	-46.0	-41.4	-47.4	-45.3	-41.9	-42.9	-39.6	-32.2	-43.9	-22.6	-23.9	-31.3	-43.4	-37.4	-40.7
Bandwidth	pm	314	266	171	169	204	224	211	359	209	200	215	202	528	222	224	351	482	203	191	224
Filter set #2																					
Performance			Broadband loss	2.2%		Interline Throughput		93%		Avg. absolute wavelength dev.			43 pm		Avg. relative bandwidth dev.			7%			
Wavelength	nm	1543.200	1543.800	1546.118	1547.373	1550.063	1550.930	1551.798	1554.013	1554.538	1556.963	1559.713	1563.173	1566.683	1570.205	1575.973	1578.268	1583.155	1584.215	1584.808	1586.220
Transmission	dB	-41.2	-14.8	-22.0	-20.8	-35.2	-38.3	-42.1	-33.8	-41.3	-39.6	-40.8	-45.1	-29.5	-37.2	-21.2	-21.4	-30.6	-42.8	-41.4	-41.5
Bandwidth	pm	323	320	183	165	193	207	217	387	207	210	220	229	496	198	234	340	507	215	214	225
Filter set #3																					
Performance			Broadband loss	0.5%		Interline Throughput		96%		Avg. absolute wavelength dev.			61 pm		Avg. relative bandwidth dev.			4%			
Wavelength	nm	1543.185	1543.803	1546.175	1547.388	1550.063	1550.983	1551.780	1554.033	1554.595	1556.980	1559.765	1563.165	1566.758	1570.268	1575.960	1578.270	1583.190	1584.223	1584.808	1586.238
Transmission	dB	-40.0	-10.9	-19.4	-20.9	-39.4	-37.1	-41.1	-38.8	-37.4	-39.5	-36.7	-41.3	-31.8	-37.3	-17.9	-20.5	-26.7	-40.4	-38.1	-39.6
Bandwidth	pm	312	281	169	173	196	203	212	335	191	202	201	215	539	200	215	336	464	200	201	245
Filter set #4																					
Performance			Broadband loss	1.8%		Interline Throughput		93%		Avg. absolute wavelength dev.			24 pm		Avg. relative bandwidth dev.			6%			
Wavelength	nm	1543.215	1543.825	1546.180	1547.368	1550.100	1550.975	1551.805	1554.035	1554.603	1557.000	1559.755	1563.150	1566.748	1570.280	1576.000	1578.248	1583.183	1584.255	1584.785	1586.245
Transmission	dB	-35.9	-12.1	-18.9	-20.6	-36.4	-36.9	-35.1	-32.4	-39.2	-38.4	-38.5	-36.8	-32.3	-36.4	-19.9	-19.8	-30.8	-33.9	-38.0	-35.9
Bandwidth	pm	304	250	156	187	209	199	201	274	205	194	213	224	473	195	217	329	483	185	215	215
Filter set #5																					
Performance			Broadband loss	2.2%		Interline Throughput		93%		Avg. absolute wavelength dev.			27 pm		Avg. relative bandwidth dev.			6%			
Wavelength	nm	1543.223	1543.848	1546.185	1547.383	1550.093	1550.973	1551.793	1554.083	1554.598	1557.020	1559.753	1563.143	1566.780	1570.260	1575.988	1578.263	1583.185	1584.258	1584.805	1586.183
Transmission	dB	-43.0	-11.7	-22.5	-23.8	-36.2	-38.7	-35.9	-38.7	-35.7	-36.6	-37.5	-38.2	-33.8	-33.3	-18.9	-22.7	-29.2	-37.4	-38.2	-37.7
Bandwidth	pm	345	277	186	191	193	213	197	337	188	193	227	207	569	184	218	355	500	213	213	220
Filter set #6																					
Performance			Broadband loss	1.8%		Interline Throughput		93%		Avg. absolute wavelength dev.			27 pm		Avg. relative bandwidth dev.			4%			
Wavelength	nm	1543.218	1543.828	1546.183	1547.338	1550.105	1550.973	1551.800	1554.028	1554.598	1556.985	1559.756	1563.115	1566.763	1570.268	1576.000	1578.225	1583.180	1584.248	1584.760	1586.233
Transmission	dB	-38.5	-12.0	-22.0	-21.2	-36.4	-39.1	-37.6	-34.6	-34.6	-35.9	-36.8	-40.7	-29.1	-36.1	-18.6	-22.5	-28.0	-31.3	-35.9	-35.0
Bandwidth	pm	316	307	180	156	210	201	197	300	212	188	199	206	520	193	228	334	455	197	198	205
Filter set #7																					
Performance			Broadband loss	3.2%		Interline Throughput		94%		Avg. absolute wavelength dev.			26 pm		Avg. relative bandwidth dev.			5%			
Wavelength	nm	1543.222	1543.839	1546.160	1547.378	1550.097	1550.981	1551.804	1554.064	1554.570	1557.014	1559.756	1563.153	1566.730	1570.243	1575.987	1578.258	1583.173	1584.263	1584.786	1586.252
Transmission	dB	-40.1	-10.5	-23.6	-21.5	-39.0	-38.5	-38.6	-38.2	-37.1	-37.7	-38.5	-38.0	-32.2	-39.0	-20.7	-22.6	-26.8	-41.4	-41.4	-38.9
Bandwidth	pm	325	254	182	151	195	204	205	317	190	197	202	237	515	215	216	329	451	235	222	218

Appendix B – Parameters for loss evaluation

Table 2. Overview of parameters for loss evaluation.

Parameter (@1550 nm)	PS1250	SM1500	GF4A	SMF-28
NA	0.12 - 0.14	0.29 - 0.31	0.30	0.14
MFD (μm)	8.8 - 10.6	4.0 - 4.5	4.0 ± 0.3	10.5
Attenuation (dB/km)	120	≤ 1.5	-	≤ 0.2
Length (m)	2.5	1	1	-
Calculated loss [dB]*	0.53 - 0.62	2.8 - 3.6	3.6	-
Measured loss [dB]**	1.85	4.85	3.03	< 0.05
CM loss [dB]***	-3.52 (at 1544.58 nm)	-0.37 (at 1544.22 nm)	-0.21 (at 1544.39 nm)	-0.93 (at 1544.07 nm)

* Calculated loss = splice loss due to angular mismatch ($< 0.5^\circ$) between fibers (patch cords and PS1250/SM1500/GF4A) with dissimilar MFD [Mil2018] + attenuation due to length of photosensitive fiber. Measured loss = measured with respect to the baseline (before FBG inscription).

** The deviation of the measured loss in PS1250 and SM1500 from the calculated loss is due to loss at fiber connectors and bending in long patch cords.

*** The CM loss is measured at the wavelength where the CM loss is most significant.

Leibniz-Institut für Astrophysik Potsdam	OH-SUPER Final Report	Friedrich-Schiller-Universität Jena
---	--------------------------	--

Appendix C – References (not listed in Sec. 4)

- [Bur2003] A. V. Buryak, K. Y. Kolossovski, and D. Y. Stepanov, "Optimization of refractive index sampling for multichannel fiber Bragg gratings," *IEEE J. Quantum Electron.*, **39**, 91–98 (2003). <https://doi.org/10.1109/JQE.2002.806202>.
- [EII2020] S. C. Ellis, J. Bland-Hawthorn, J. S. Lawrence, A. J. Horton, R. Content, M. M. Roth, N. Pai, R. Zhelem, S. Case, E. Hernandez, S. G. Leon-Saval, R. Haynes, S. S. Min, D. Giannone, K. Madhav, A. Rahman, C. Betters, D. Haynes, W. Couch, L. J. Kewley, R. McDermid, L. Spitler, R. G. Sharp, and S. Veilleux, "First demonstration of OH suppression in a high-efficiency near-infrared spectrograph," *Monthly Notices of the Royal Astronomical Society* **492**, 2796–2806 (2020). <https://doi.org/10.1093/mnras/staa028>.
- [Goe2018] T. A. Goebel, G. Bharathan, M. Ams, M. Heck, R. G. Krämer, C. Matzdorf, D. Richter, M. P. Siems, A. Fuerbach, and S. Nolte, "Realization of aperiodic fiber Bragg gratings with ultrashort laser pulses and the line-by-line technique," *Optics Letters* **43**, 3794–3797 (2018). <https://doi.org/10.1364/OL.43.003794>
- [Goe2020] T. A. Goebel, M. Heusinger, R. G. Krämer, C. Matzdorf, T. O. Imogore, D. Richter, U. D. Zeitner, and S. Nolte, "Femtosecond inscription of semi-aperiodic multi-notch fiber Bragg gratings using a phase mask," *Optics Express* **28**, 35682 (2020).
- [Her2022] E. Hernandez, A. Günther, S-M. Bauer, C. D. Guzmán, C. Sandin, A. Stoll, S. Vješnica, K. Madhav, M. M. Roth, "System integration of the Potsdam Arrayed Waveguide Spectrograph (PAWS)," *Proc. SPIE 12184, Ground-based and Airborne Instrumentation for Astronomy IX*, 121841O (2022). <https://doi.org/10.1117/12.2627318>.
- [Mad2023] K. Madhav, A. Günther, E. Hernandez, S. Vješnica, D. Bodenmüller, A. Stoll, C. Sandin, H. A. Yıldırım, M. M. Roth, "PAWS and POCO: NIR Astrophotonic Instruments for Astronomy," *Astronomische Nachrichten* **344**, e20230089 (2023). <https://doi.org/10.1002/asna.20230089>.
- [Mei1950] A.B. Meinel, II, "OH Emission Bands in the Spectrum of the Night Sky. II." *ApJ* **112**, 120–130 (1950). <https://doi.org/10.1086/145296>.
- [Mil2018] G. A. Miller and H. M. Coombs, "Low Loss Splices to Dissimilar Optical Fibers," Naval Research Laboratory, Report No. NRL/MR/5675–18-9822 (2018). <https://apps.dtic.mil/sti/html/tr/AD1064067/>
- [Rah2020] A. Rahman, K. Madhav, and M. M. Roth, "Complex phase masks for OH suppression filters in astronomy: part I: design," *Opt. Express* **28**, 27797–27807 (2020). <https://doi.org/10.1364/OE.402989>.
- [Rou2000] P. Rousselot and C. Lidman, "Night-sky spectral atlas of OH emission lines in the near-infrared," *Astronomy and Astrophysics* **354**, 1134 (2000).
- [Ryp2024] J. J. Rypalla, "On the large quantity fabrication and reproducibility of all-fiber photonic lantern," Master's thesis, University of Potsdam, 2024 (available on request).
- [Ska2003] J. Skaar and O. Waagaard, "Design and characterization of finite-length fiber gratings," *IEEE J. Quantum Electron.*, **39**, 1238–1245 (2003). <https://doi.org/10.1109/JQE.2003.817581>.
- [Tho2012] J. Thomas, C. Voigtländer, R. G. Becker, D. Richter, A. Tünnermann, and S. Nolte, "Femtosecond pulse written fiber gratings: a new avenue to integrated fiber technology," *Laser & Photonics Reviews* **6**, 709–723 (2012). <https://doi.org/10.1002/lpor.201100033>
- [Tri2013] C. Q. Trinh, S. C. Ellis, J. Bland-Hawthorn, J. S. Lawrence, A. J. Horton, S. G. Leon-Saval, K. Shortridge, J. Bryant, S. Case, M. Colless, W. Couch, K. Freeman, H-G Löhmannsröben, L. Gers, K. Glazebrook, R. Haynes, S. Lee, J. O'Byrne, S. Miziarski, M. M. Roth, B. Schmidt, C. G. Tinney, and J. Zheng "GNOSIS: The first instrument to use fiber Bragg gratings for OH suppression," *The Astron. J.* **145**, 51–64 (2013). <https://doi.org/10.1088/0004-6256/145/2/51>.